UHASSELT
KNOWLEDGE IN ACTION

Maastricht University

Faculty of Medicine and Life Sciences
School for Life Sciences
Master of Biomedical Sciences

Master's thesis

Dental pulp stem cells as suicide gene carriers for oral squamous cell carcinoma treatment: investigating gap junction formation in a co-culture model

Edita Lokmani

Thesis presented in fulfillment of the requirements for the degree of Master of Biomedical Sciences, specialization Molecular Mechanisms in Health and Disease

SUPERVISOR :

Prof. dr. Esther WOLFS

MENTOR :

Mevrouw Jolien VAN DEN BOSCH

2022
2023

Transnational University Limburg is a unique collaboration of two universities in two countries: the University of Hasselt and Maastricht University.

UHASSELT
KNOWLEDGE IN ACTION

www.uhasselt.be
Universiteit Hasselt
Campus Hasselt:
Martelarenlaan 42 | 3500 Hasselt
Campus Diepenbeek:
Agoralaan Gebouw D | 3590 Diepenbeek

Faculty of Medicine and Life Sciences
School for Life Sciences
Master of Biomedical Sciences

Master's thesis

Dental pulp stem cells as suicide gene carriers for oral squamous cell carcinoma treatment: investigating gap junction formation in a co-culture model

Edita Lokmani

Thesis presented in fulfillment of the requirements for the degree of Master of Biomedical Sciences, specialization Molecular Mechanisms in Health and Disease

SUPERVISOR :

Prof. dr. Esther WOLFS

MENTOR :

Mevrouw Jolien VAN DEN BOSCH

Dental pulp stem cells as suicide gene carriers for oral squamous cell carcinoma treatment: investigating gap junction formation in a co-culture model*

Lokmani E[1], Van den Bosch J[1], and Wolfs E[1]

[1]FIERCE Lab, Biomedical Research Institute, Hasselt University, Agoralaan Building C – B3590 Diepenbeek

*Running title: *DPSC-mediated suicide gene therapy for OSCC*

To whom correspondence should be addressed: Esther Wolfs, Tel: +32 11 26 92 96; Email: esther.wolfs@uhasselt.be

Keywords: Oral squamous cell carcinoma; dental pulp stem cells, suicide gene therapy; Herpes Simplex Virus type 1 thymidine kinase/ganciclovir system; gap junctions

ABSTRACT

Oral squamous cell carcinoma (OSCC) is the predominant type of head and neck cancer. Despite advances in current treatment options, the survival rate of these patients has not significantly improved. These therapies are also associated with severe side effects. To reduce side effects and save healthy tissue, we aim to develop a suicide gene therapy based on the herpes simplex virus type 1 thymidine kinase (HSV1-TK)/ganciclovir (GCV) system using dental pulp stem cells (DPSC) as a carrier. Characterization of DPSC was researched using immunocytochemistry (ICC), quantitative polymerase chain reaction (qPCR), and bioluminescence imaging (BLI). Gap junction formation between DPSC and OSCC and cell viability were investigated via ICC and alamarBlue assay respectively in 2D and 3D co-cultures. Our results demonstrated that DPSC of five donors were transduced correctly with the lentiviral construct containing HSV1-TK. Additionally, the presence of connexin 43 between DPSC and OSCC was observed, indicating potential gap junction formation between both cell types. Finally, the killing efficiency of the HSV1-TK$^+$/GCV system was approved in a 2D and 3D co-culture. In conclusion, our findings show that HSV1-TK/GCV suicide gene therapy, carried by DPSC, is a promising strategy for OSCC *in vitro*. However, further research is essential to investigate the use of this system *in vivo*.

INTRODUCTION

Cancer is the second leading cause of mortality worldwide. It is described as a large group of diseases in which abnormal cells divide uncontrollably and can invade surrounding tissues and organs. The spreading of cancer cells to other body parts is defined as metastasizing and is the major cause of cancer death. Risk factors that may increase cancer development are genetic abnormalities, age, and external influences, such as tobacco use, alcohol consumption, unhealthy diet, lack of physical activity, and air pollution (1). In 2000, Hanahan and Weinberg described six hallmarks of cancer: sustaining proliferative signaling, evading growth suppressors, activating invasion and metastasis, enabling replicative immortality, inducing angiogenesis, and resisting cell death (2). Normal cells acquire these properties, allowing them to become tumorigenic and ultimately malignant. Understanding cancer formation and malignant progression is essential in developing treatments. As cancer

research in the past decade has evolved, two emerging hallmarks, reprogramming of energy metabolism and evading immune destruction, were added. Furthermore, two enabling characteristics were described: tumor-promoting inflammation and genome instability and mutation (3). Additionally, unlocking phenotypic plasticity, non-mutational epigenetic reprogramming, polymorphic microbiomes, and senescent cells were proposed by Hanahan as possible core cancer properties in January 2022 (4).

One of the most prevalent types of this disease is **head and neck cancer** (HNC), the seventh most common cancer type worldwide (5). It refers to malignancies in the paranasal sinuses, nasal and oral cavity, pharynx, and larynx. The main risk factors are tobacco exposure, chronic heavy alcohol consumption, and human papillomavirus (HPV) infection (6, 7). Approximately 90% of head and neck cancers arise from the stratified squamous epithelium, defining them as **oral squamous cell carcinoma** (OSSC) (8). The histological progression of OSCC toward an invasive tumor starts with differentiation from normal mucosal epithelial cells into mucosal epithelial cell hyperplasia, followed by dysplasia, carcinoma *in situ*, and invasive carcinoma (9). The histological evaluation is used in the diagnosis of head and neck cancers after fine-needle aspiration of a submucosal lesion and/or a suspicious lymph node (10). After a cancer diagnosis is confirmed, PET-CT imaging is used to determine the cancer stage, which is important in the prognosis. Besides cancer stage, the tumor location, age, and overall health of the patient also play a crucial role (11). Furthermore, it is known that the prognosis of head and neck cancers associated with HPV has a better outcome (12, 13). Despite advancements made in current treatment options, including surgery, radiotherapy, and chemotherapy, they can result in significant side effects. For instance, surgical restriction may lead to swallowing or speaking difficulties, and altered aesthetics, while radiotherapy can induce skin irritation. Additionally, chemotherapy may cause hair loss, nausea, and fatigue. Also, clinical symptoms such as dysphagia, odynophagia, hoarseness, mucosal irregularities, mouth ulcer, and oral pain may have an impact on the life quality. These consequences can be physically and emotionally challenging for patients, making it crucial to search for alternative treatment options. Moreover, the disease's five-year survival rate has not improved over time due to the limited therapeutic effect and remains around 50% (14). To overcome these limitations, new therapeutic strategies for OSCC are being investigated. Therefore, interest in alternative therapies such as immunotherapy, targeted drug therapy, and gene therapy has increased. These treatment approaches aim to specifically target cancer cells, preserving healthy cells and potentially reducing the adverse effects (15). Immunotherapy, such as checkpoint inhibitors and monoclonal antibodies, enhances the patient's immune system in recognizing and attacking malignant cells (16-18). On the other hand, targeted drug therapy, including epidermal growth factor receptor (EGFR) and vascular endothelial growth factor (VEGF) inhibitors, blocks cancer cell proliferation by using drugs that target mutated genes or proteins which are responsible for tumor cell growth (19). In this study, we will focus on gene therapy in the treatment of OSCC, which will be discussed further in the following section.

Cancer gene therapy aims to treat cancer by introducing therapeutic genes into

malignant cells and ceasing tumor growth. OSCC is a good candidate for this therapeutic approach since primary and recurrent lesions can be easily targeted by the agent. Moreover, this therapy is divided into three types: (1) corrective gene therapy, (2) toxin/apoptosis-inducing gene therapy, and (3) suicide gene therapy (20). In the first class, therapeutic genes are introduced to correct mutated genes responsible for cancer development. For example, a mutation in tumor suppressor genes can cause uncontrolled cell division, leading to tumor formation (21, 22). Additionally, this therapy can treat cancer caused by genetic interfering agents such as siRNA and miRNA by binding to these agents and ultimately blocking their activity (23, 24). In toxin/apoptosis-inducing gene therapy, a gene that produces a toxin protein (e.g. diphtheria toxin or TNF-α) is delivered to cancer cells, causing apoptosis. However, the problem with the therapies described above is that only cells in which the therapeutic gene is introduced will be affected. Therefore, cancer cells in the tumor core are not targeted (25). One approach to overcome this obstacle is via **gene-directed enzyme prodrug therapy (GDEPT)**, also known as suicide gene therapy, in which cancer cells are transduced with a gene coding for an enzyme (suicide gene), followed by the administration of a non-toxic prodrug. After cancer cells take up the suicide gene, the prodrug converts to its toxic variant. This will eventually lead to cancer cell death (20).

A major advantage of suicide gene therapy is that toxic metabolites are transferred from transduced cells to surrounding non-transduced cells. This promotes the extension of the cytotoxic effect, making it possible to target the tumor core. This phenomenon is defined as the **bystander effect** and can be established via three different mechanisms: (1) endocytosis, (2) distant bystander effect, and (3) gap junctional intercellular communication (GJIC) (20). In the first mechanism, non-transduced cells can take up apoptotic bodies secreted by transduced cells via endocytosis (26). Secondly, this phenomenon can also be established via the distant bystander effect that involves the activation of the immune system. When tumor cells undergo apoptosis, tumor-associated antigens can be released, which activate immune cells, resulting in the elimination of tumor cells (27, 28). Finally, the main mechanism works through the diffusion of the toxic metabolites from transduced cells to non-transduced cells via GJIC (29). Gap junctions are integral membrane complexes of connexin proteins that allow cell communication. They allow the transfer of ions and small molecules between neighboring cells. The most prevalent connexin in human gap junctions is connexin 43 (Cx43) (30, 31).

The two main **enzyme/prodrug systems** used in suicide gene therapy include cytosine deaminase/5-fluorocytosine (CD/5-FC) and herpes simplex virus type I- thymidine kinase/ganciclovir (HSV1-TK/GCV) (32). In the CD/5-FC system, the enzyme CD converts 5-FC to 5-fluorouracil (5-FU), a small molecule that can easily diffuse to a neighboring cell. 5-FU is converted to several metabolites by intracellular enzymes, inhibiting thymidylate synthase and this will eventually cause cell death (33). However, the therapeutic dose of 5-FU is associated with adverse effects such as mucositis (34). This study focuses on the **HSV1-TK/GCV system**, which is the most used suicide gene therapy system in preclinical studies (20). HSV1-TK is an enzyme derived from the herpes simplex virus type I. Unlike cytosolic TK, HSV1-TK has a broad substrate

specificity, such as pyrimidines, purines, and their analogs. GCV is an example of a purine analog and has a 1000-fold higher affinity to HSV1-TK compared to cytosolic TK (35). This non-toxic prodrug is normally used to treat viral infections, especially those originated from the herpesvirus family, such as cytomegalovirus (CMV) infections (36). In the HSV1-TK/GCV system, GCV is phosphorylated by HSV1-TK to GCV monophosphate and subsequently converted into GCV triphosphate by intracellular enzymes (37). GCV induces apoptosis by incorporating into the replicating DNA, leading to single-strand breaks and eventually termination of DNA elongation (38). However, the high GCV doses required for a therapeutic effect can be toxic for healthy cells. To overcome this obstacle, *Black et al. (2001)* created HSV1-TK mutants (SR11, SR26, and SR39) via a semi-random sequence mutagenesis approach. The advantage of these mutants is an enhanced cell death approach and a lower required amount of GCV for the desired effect (39). In this research, the HSV1-sr39TK was used.

In addition, HSV1-TK can also be used as a reporter gene in molecular imaging techniques. Radiolabeled enzymes are used as a substrate for HSV1-TK. Transduced cells are able to phosphorylate these enzymes, which are then trapped in these cells (40). Subsequently, the radiolabeled enzyme can be detected via positron emission tomography (PET) imaging. This approach can be implemented to image and measure HSV1-TK gene expression *in vivo* (41). Also, the HSV1-TK/GCV system can be employed as a possible safety switch for the use of stem cells with an unfavorable safety profile regarding uncontrolled cell proliferation (42).

Besides the enzyme and prodrug, the **delivery system** is also a crucial factor for the therapy. The suicide gene can be integrated into vectors and subsequently transported to the tumor cells. However, the development of a suitable delivery system remains a challenge. Important characteristics of a good system include low toxicity/immunogenicity and high transfection efficiency, tissue specificity, and cost-effectiveness (43). Currently, the most common delivery system is via viruses (44). Nevertheless, several disadvantages, such as triggering the immune response and insertional mutagenesis, limit the clinical relevance of these systems (45). Therefore, extensive research is evolving on non-viral gene delivery. Cell-based delivery systems, such as the use of mesenchymal stem cells (MSC), could be a potential solution to overcome these issues (46). MSC are a type of adult stem cells and are characterized by the presence of different surface markers, including CD90, CD105, and CD73 and must lack expression of CD45, CD34, CD14 or CD11b, CD79α or CD19, and HLA-DR surface (47). Additionally, previous studies have shown that MSC are a promising suicide gene delivery system (48, 49). However, to obtain enough MSC yield, they must be isolated via bone marrow aspiration, which is an invasive approach (50). To overcome this limitation, dental pulp stem cells (DPSC) can be used since they are isolated from the dental pulp of third molars, which is a less invasive isolation strategy (51). These adult stem cells have mesenchymal stem cell-like properties. They are beneficial in cancer treatment since they have immunosuppressive properties such as secretion of immunosuppressive cytokines, a great proliferation potential, and active migration toward tumor cells via chemotactic mediators secreted by cancer cells (52, 53). In this project, DPSC are used in combination with the HSV1-TK/GCV suicide gene therapy system.

As described earlier, functional gap junctions enable intercellular communication between cells, resulting in the bystander effect. Our project aims to investigate if gap junctions between DPSC and OSCC are functional and will result in the bystander effect after ganciclovir administration. In this way, we want to develop a more targeted treatment for patients with OSCC leading to fewer side effects and, eventually, apply this technique to other cancer types. Therefore, we **hypothesize** that phosphorylated ganciclovir is transferred from HSV1-TK expressing DPSC to OSCC via gap junctions, causing apoptosis in both cell types *in vitro* (**figure 1**). We will investigate this by first characterizing DPSC via ICC, qPCR, and BLI. Secondly, we will determine the presence of gap junctions in 2D and 3D co-cultures via ICC. Finally, an alamarBlue assay will be performed to investigate cell death in 2D and 3D co-cultures after GCV administration.

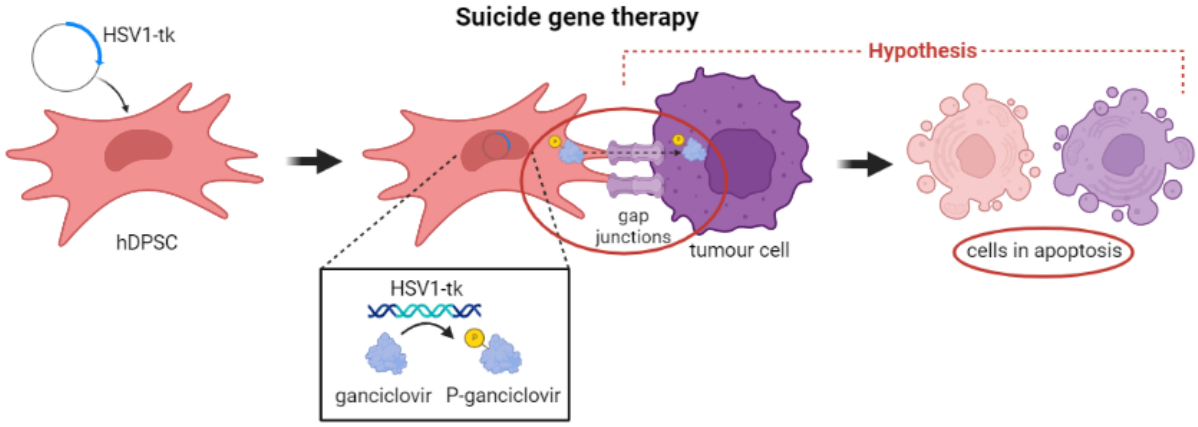

Figure 1: Graphical representation of the mechanism behind the HSV1-TK/GCV system in the eradication of DPSC and OSCC. DPSC will be transduced with a lentiviral vector containing the HSV1-TK gene. Preliminary data has shown that DPSC migrate toward OSCC and form gap junctions. HSV1-TK is able to convert GCV into its toxic metabolite, which causes apoptosis in cells. It is hypothesized that toxic P-GCV will be transferred from DPSC to OSCC via gap junctions and will eventually lead to apoptosis in both cell types. *DPSC, dental pulp stem cells; OSCC, oral squamous cell carcinoma; HSV1-TK, Herpes Simples Virus type 1 Thymidine Kinase; P, phosphorylated. Figure made in BioRender.*

MATERIALS AND METHODS

Cell isolation and culturing – DPSC were isolated from dental pulp tissue derived from third molars of donors at Ziekenhuis Oost-Limburg (ZOL, Genk, Belgium) as previously described by *Hilkens P. et al. (2013)*. DPSC were cultured in α-Minimal Essential Medium (Sigma-Aldrich) supplemented with 10% fetal calf serum (FCS). OSCC (UM-SCC-14C, CLS cell lines service, Eppelheim, Germany, CVCL_7721) were cultured in Dulbecco's Modified Eagle Medium/Nutrient Mixture F-12 Ham (Sigma-Aldrich) supplemented with 5% FCS. Both media were supplemented with 1% penicillin-streptomycin (Sigma-Aldrich), 2 mM L-glutamine (Sigma Aldrich) at 37°C under 5% CO_2 in a humidified area. For the formation of co-cultures, DPSC and OSCC were cultured in a 1:1 ratio in OSCC growth medium. 2D co-cultures for ICC consisted of $6x10^4$ cells/cm^2 and for viability assays of $1x10^4$ cells/cm^2. For 3D cultures (hydrogels), $8x10^4$ cells/µL were used for ICC and $5x10^4$ cells/µL for Alamar blue. For ICC co-cultures, DPSC were pre-

stained with ViaFluor® 488 (Biotium, Fremont, United States, 1:4000) and OSCC with ViaFluor® 405 (Biotium, Fremont, United States, 1:1000) according to the manufacturer's protocol. To ensure gap junction formation, experiments were started two days after reaching 100% confluency. Hydrogels were composed of 10% Minimum Essential Medium Eagle (MEM, Sigma-Aldrich, St-Louis, MO, USA) and 80% type 1 rat tail collagen (First Link, Wolverhampton, United Kingdom) (5 mg/ml in 0.6% acetic acid), followed by neutralization with sodium hydroxide.

Vector construct of transduced DPSC – HSV1-TK$^+$ DPSC were transduced with the vector via lentiviral transduction following the protocol of Tiscornia *et al*. The vector consisted of an EF-1α promoter, HSV1-sr39TK, a T2A linker sequence, His-FLAG tagged Firefly luciferase (FLuc), IRES linker sequence, and a puromycin resistance cassette.

Immunocytochemistry (ICC) – DPSC and 2D co-cultures were seeded on glass coverslips with a density of 3x10^4 cells/cm^2. 2D cultures were fixed with Unifix (VWRK4031-9010, Klinipath, Olen, Belgium) for 20 min, 3D cultures for 40 min. For intracellular staining, cells were permeabilized with 0.05% Triton X-100 in PBS for 30 min at 4°C. To prevent unspecific binding of the antibodies, 2D and 3D cultures were incubated for 1 h and 3 h respectively with 10% protein block in PBS (Agilent Dako). Subsequently, primary antibodies (**supplementary table 1**) were incubated overnight at 4°C. Negative control samples without primary antibody were included in the experiments. Thereafter, 2D cultures were incubated for 2 h and 3D cultures for 6 h with secondary antibodies (**supplementary table 2**) diluted in PBS at room temperature. Nuclei were counterstained with 4,6-diamidino-2- phenylindole (DAPI, 1/10 000, Boehringer Mannheim GmbH, Germany) if nuclear visualization was preferred. Glass coverslips were mounted with mounting media (Fluoromount-G™, Invitrogen, Thermo Fisher Scientific) and images were obtained at a magnification of 40x with the Leica DM4000 B microscope (Leica Microsystems, Wetzlar, Germany) or the confocal Zeiss LSM 880 (Zeiss, Zaventem, Belgium). Quantitative analyses were performed using ImageJ software (version 2.1.0/1.53t). Fluorescent signals were expressed as the integrated density, which was calculated by the formula: $integrated\ density = \frac{area\ x\ mean}{amount\ of\ cells}$. Five pictures per staining were taken.

Quantitative polymerase chain reaction (qPCR) – DPSC were seeded on a 24-well plate with a density of 3,5x10^4 cells/cm^2. RNA was isolated via TRIzol™ (Invitrogen, Thermo Scientific) reagent method using QIAzol (Qiagen Sciences) according to the manufacturer's protocol. Purity and contamination was determined via NanoDrop 2000 Spectrophotometer (Isogen Life Science, Thermo Fisher Scientific). RNA samples were diluted to 7.5 ng/µl and qScript cDNA SuperMix (Quantabio, Leuven, Belgium) was added to the samples to synthesize cDNA. qPCR was performed using cDNA samples in a 10 µl reaction mixture containing Fast SYBR™ Green Master Mix (Applied Biosystems, Thermo Fisher Scientific) and primer pairs listed in **supplementary table 3**. Ct-values were obtained using QuantStudio 3 (Applied Biosystems, Thermo Fisher Scientific). A holding stage at 95 °C for 20 s, cycling stage (40x) at 95 °C for 3s and at 60 °C for 30 s, and melt curve stage at 95 °C for 15 s, at 60 °C for 60 s, and 95 °C for 15 s was conducted.

Results were analyzed via QuantStudio software. Ct-values of target genes were normalized relative to the Ct-values CYCA and YWHZ.

Bioluminescence imaging (BLI) – $5x10^3$ cells/cm² were seeded in a black 96-well plate with clear bottom. FLuc activity was measured with the ONE-Glo™ Luciferase Assay System (Promega Corporation) according to the manufacturer's instructions and analyzed via the CLARIOstar® PLUS plate reader (BMGLABTECH, De Meern, The Netherlands).

Cell viability assessment after ganciclovir (GCV) administration – Five or six different GCV (Cymevene®) concentrations (ranging from 0.01 µM to 1000 µM) were administered to 2D and 3D co-cultures of HSV1-TK$^-$ DPSC/OSCC and HSV1-TK$^+$ DPSC/OSCC respectively every other day. OSCC medium was used as a negative control and milli-Q water was used as a positive control. After 7 and 14 days for 2D and 3D co-cultures respectively, alamarBlue was added in a 1/10 ratio, diluted in phenol red-free medium (Sigma-Aldrich). After 4h incubation for 2D and overnight incubation for 3D co-cultures, the samples were transferred to a black/clear bottom 96 well-plate and analyzed via the CLARIOstar® PLUS plate reader (BMGLABTECH, De Meern, The Netherlands).

Statistical analysis – Data were analyzed using GraphPad Prism 9.5.0 (730). The Shapiro-Wilk test was used to test for normal distribution. To determine significance, a paired t-test, one-way ANOVA with Bonferroni's or Dunnett's multiple comparisons test was used when data passed the normality test, whereas a Wilcoxon matched-pairs signed rank test was used when data were not normally distributed. Significance level was set at $P < 0.05$. Outliers were determined via the Grubbs' test. Data were represented as mean±SEM.

RESULTS

Characterization of the HSV1-TK$^+$ DPSC and investigation of interpatient variability

In this research, our first aim was to determine the transduction efficiency of the DPSC with the HSV1-TK gene and to investigate the interpatient variability between five donors. Since the vector comprises the HSV1-TK, FLAG-tag, and His-tag genes, ICC was performed to determine if DPSC were transduced correctly by investigating the protein expression of these genes. Our results showed that the mean integrated densities of HSV1-TK, FLAG-, and His-tag were significantly higher in the HSV1-TK$^+$ cells compared to the HSV1-TK$^-$ cells in all donors (**figure 2A**). **Figure 2B** shows representative images of transduced cells expressing HSV1-TK, FLAG-, and His-tag proteins, whereas non-transduced cells did not express these proteins. Our findings also demonstrated that the mean integrated density of HSV1-TK was notably higher compared to FLAG- and His-tag.

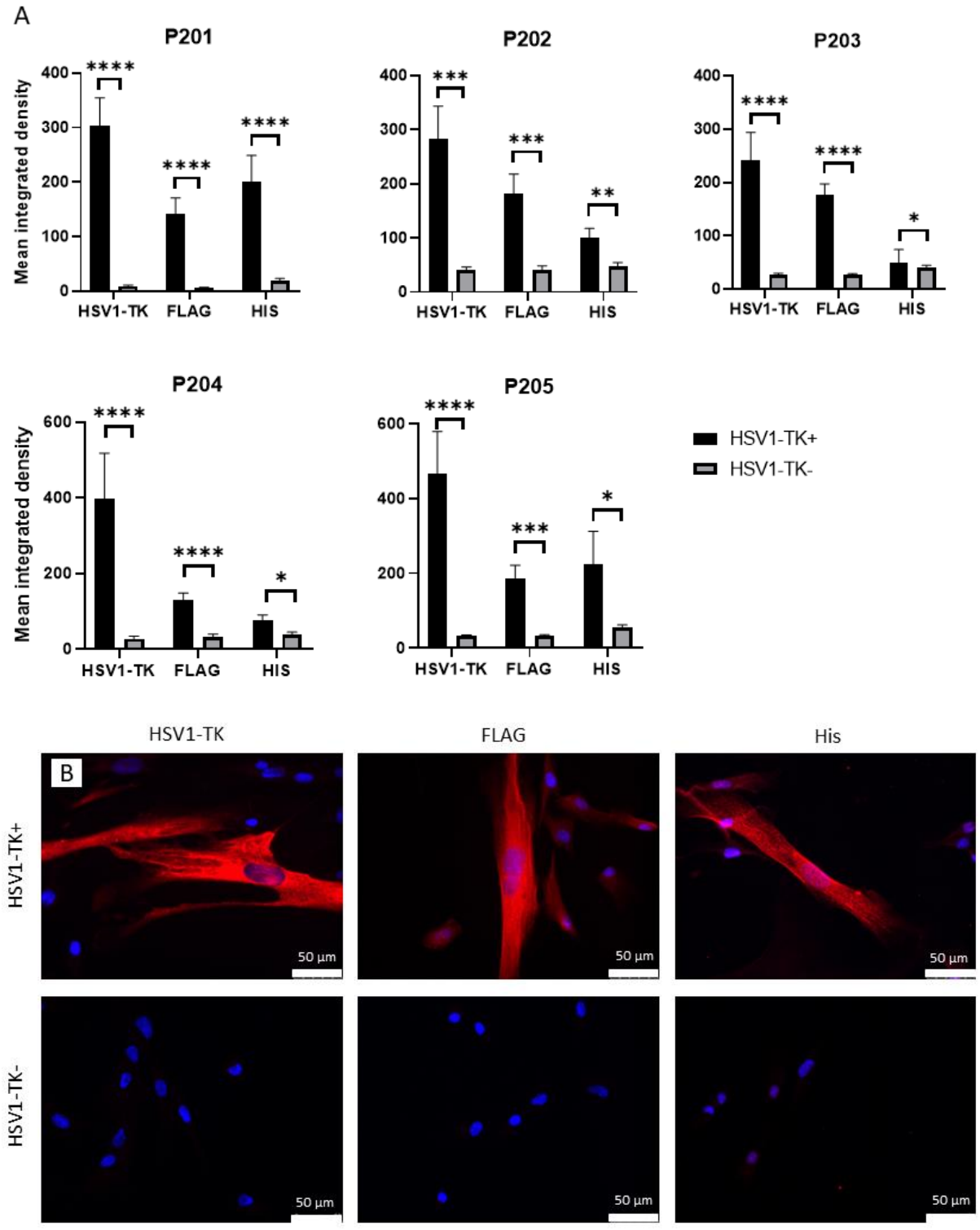

Figure 2: DPSC of all donors were correctly transduced with the vector construct containing HSV1-TK, FLAG-tag, and His-tag. (A) Quantification of the integrated density of HSV1-TK, FLAG, and His in transduced (+) DPSC compared to non-transduced (-) DPSC of all five donors (P201-P205) (n=3). *p<0.05, **p<0.01, ***p<0.001, ****p<0.0001. Paired t-test (P202-P205, FLAG) or Wilcoxon matched-pairs signed rank test (P201 FLAG and P201-205, HSV1-TK and His) was used. **(B)** Representative images of immunocytochemical staining of HSV1-TK, FLAG, and His (red) of transduced (top) and non-transduced (bottom) DPSC obtained with the Leica DM4000 fluorescent microscope at 40x. Nuclei (blue) were stained with DAPI. Scalebar, 50 µm. Data are represented as mean±SEM. *HSV1-TK, Herpes Simplex Virus type 1 Thymidine Kinase.*

Moreover, mRNA expression levels of the HSV1-TK gene were measured via qPCR to characterize the DPSC. The mRNA levels of the HSV1-TK gene in transduced cells are shown in **figure 3B**. Non-transduced DPSC had no HSV1-TK mRNA expression in the different donors. Since the vector construct also contains a Firefly luciferase (FLuc) gene, it is possible to measure bioluminescence. Higher bioluminescence signals were observed in transduced DPSC compared to non-transduced DPSC (data not shown).

To determine if the HSV1-TK gene was expressed evenly in all donors, the normalized integrated density and mRNA expression levels of transduced DPSC were compared between five donors. No significant differences were obtained between all donors when looking at the normalized integrated density of HSV1-TK, FLAG, and His-tag (**figure 3A**). Normalized integrated density indicates the difference in the mean integrated density of transduced and non-transduced DPSC (Δpositive - Δnegative). In **figure 3B**, qPCR data of transduced DPSC of P201-P205 is shown. Ours results indicated that the HSV1-TK mRNA expression levels of P202 and P205 differed significantly from other donors.

To determine if DPSC transduction has an influence on the stem cell characteristics, mRNA levels of transduced and non-transduced cells were compared. The mRNA expression of three positive (CD90, CD105, and CD73) and two negative (CD45 and CD34) stem cell markers were researched. The mRNA levels of CD90, CD105, and CD73 in transduced and non-transduced DPSC between five donors did not differ significantly (**Figure 3C-E**). Additionally, no mRNA expression of CD45 and CD34 was measured. Therefore, statistical analysis could not be performed.

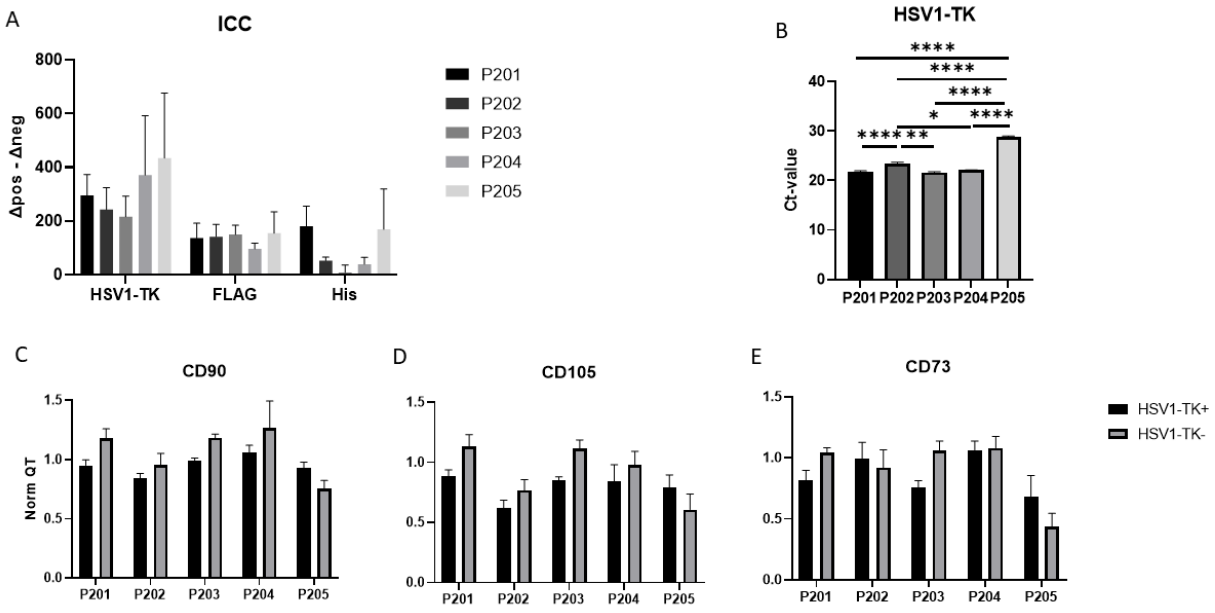

Figure 3: Interpatient variability assessment via ICC and qPCR. (A) No significant differences between all five donors in all three proteins were obtained when comparing the difference in mean integrated density of transduced and non-transduced DPSC (Δpositive - Δnegative) (n=3). **(B)** Ct-values of HSV1-TK gene in P202 and P205 were significantly different from other donors (n=3). Relative mRNA expression (norm QT) of positive stem cell markers **(C)** CD90, **(D)** CD105, and **(E)** CD73 between transduced (HSV1-TK$^+$) and non-transduced

(HSV1-TK$^-$) DPSC was not significantly different in all donors (n=3). *p<0.05, **p<0.01, ****p<0.0001. One-way ANOVA with Bonferroni's multiple comparisons test (A-E) was used. Data are represented as mean±SEM. *ICC, immunocytochemistry; HSV1-TK, Herpes Simplex Virus type 1 Thymidine Kinase.*

Gap junction formation between DPSC and OSCC in 2D and 3D *in vitro* co-cultures

The second aim of this research was to determine the presence of gap junctions between DPSC and OSCC. As described earlier, Cx43 expression indicates the formation of gap junctions between adjacent cells. To this end, ICC staining of Cx43 (magenta) was performed in a 2D (**figure 4**) and 3D (**figure 5**) co-culture model where cytoplasmic staining can distinguish DPSC (blue) and OSCC (yellow). It was observed that DPSC and OSCC were densely located together in a 2D co-culture. Additionally, Cx43 was highly expressed on the surface of DPSC and in a lesser extent in OSCC. Furthermore, the presence of Cx43 was also observed at the junction between DPSC and OSCC in both co-cultures, indicated with a white arrow. Cx43 expression was seemingly more intense at these junctions.

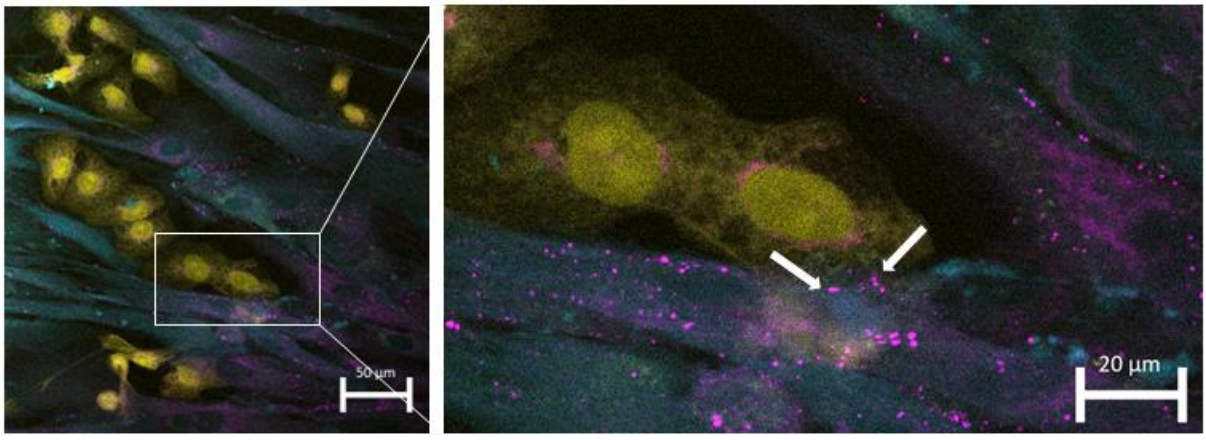

Figure 4: Potential presence of gap junctions between DPSC and OSCC in a 2D *in vitro* co-culture. Immunocytochemical staining of gap junction formation (Cx43, magenta) between DPSC (ViaFluor® 488, blue) and OSCC (ViaFluor® 405, yellow), indicated with a white arrow, obtained with confocal Zeiss LSM 880 at 40x. Scalebar, 50 µm (left) and 20 µm (right). *DPSC, dental pulp stem cells; OSCC, oral squamous cell carcinoma; Cx43, connexin 43.*

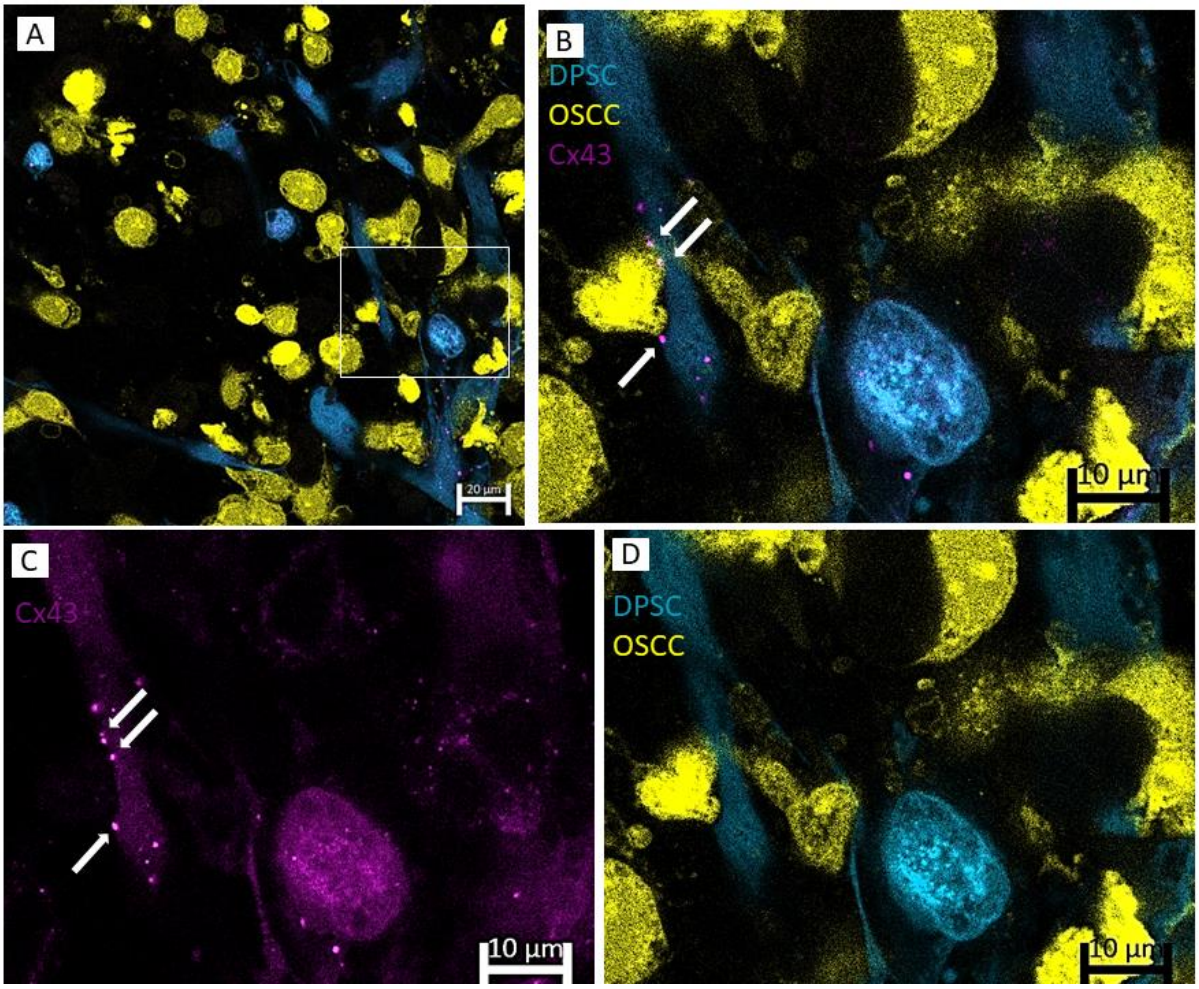

Figure 5: Potential presence of gap junctions between DPSC and OSCC in a 3D *in vitro* co-culture. Immunocytochemical staining of gap junction formation (Cx43, magenta) between DPSC (ViaFluor® 488, blue) and OSCC (ViaFluor® 405, yellow), indicated with a white arrow, obtained with confocal Zeiss LSM 880 at 40x. Scalebar, 20 µm (A) and 10 µm (B-D). *DPSC, dental pulp stem cells; OSCC, oral squamous cell carcinoma; Cx43, connexin 43.*

Killing efficiency of HSV1-TK$^+$ DPSC in a DPSC/OSCC 2D and 3D co-culture model with different GCV concentrations

As explained earlier, the presence of Cx43 between DPSC and cancer cells indicates gap junction formation. Additionally, it is expected that cytotoxic GCV can be passed through these gap junctions in an efficient way. Nevertheless, the cell-killing ability of HSV1-TK$^+$ DPSC still has to be validated. To this end, five or six different GCV concentrations were administered to 2D and 3D co-cultures of DPSC and OSCC respectively, ranging from 0.01 µM to 1000 µM. For both co-cultures, an alamarBlue assay was performed to investigate cell viability (**figure 6**). As a negative control, co-cultures were constructed with non-transduced cells to investigate the cytotoxicity of GCV. Our results showed that cell viability of HSV1-TK$^-$/OSCC co-cultures treated with GCV concentrations ranging from 0.01 µM to 1000 µM in both 2D and 3D co-cultures did not differ significantly from the untreated (0 µM) cells.

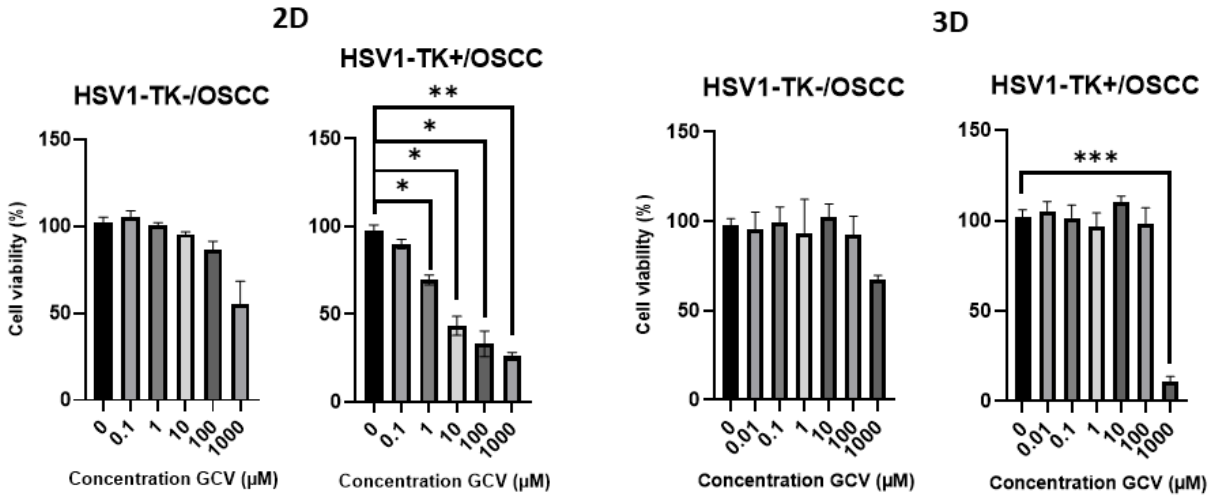

Figure 6: Cell viability assessment of 2D and 3D DPSC/OSCC co-cultures after GCV administration. 2D (n=4) and 3D (n=3) co-cultures were treated with five and six different GCV concentrations respectively, ranging from 0.01 µM to 1000 µM. Co-cultures were treated every other day and alamarBlue assay was performed after 7 and 14 days respectively for 2D and 3D co-cultures. No significant differences were observed in 2D and 3D HSV1-TK$^-$/OSCC co-cultures. Cell viability of 2D HSV1-TK$^+$/OSCC decreased significantly from 1 µM, whereas cell viability of 3D HSV1-TK$^+$/OSCC was significantly different from 1000 µM. *p<0.05, **p<0.01, ***p<0.001. One-way ANOVA with Dunnett's multiple comparisons test was used. Data are represented as mean±SEM. *HSV1-TK, Herpes Simplex Virus type 1 Thymidine Kinase; OSCC, oral squamous cell carcinoma.*

In the HSV1-TK$^+$/OSCC co-cultures, the killing efficiency of the suicide gene system was investigated. In the transduced 2D co-cultures, a significant concentration-dependent decrease in cell viability was observed. Untreated (0 µM) cells (97.80% ± 3.08) differed significantly from cells treated with 1 µM (69.52% ± 2.73), 10 µM (43.36% ± 5.40), 100 µM (33.12% ± 7.29), and 1000 µM (25.93% ± 2.23) GCV. In the transduced 3D co-cultures, a significant difference between untreated (0 µM) cells and cells treated with 1000 µM (102.23% ± 3.73 vs. 10.82% ± 2.91) GCV was observed.

DISCUSSION

HNC is the 7th most common cancer worldwide, with a global prevalence of around 3% of all cancers and its incidence continues to rise (5). The increasing rate is associated with the rising incidence of HPV infection in the USA and Europe, while in Southeast Asia and Asia-Pacific regions it is linked to chewing of betel nut (54, 55). OSCC are the most widespread type of HNC, accounting for approximately 90% of the disease. Despite the advances made in therapy, conventional treatment options, including surgery, radiotherapy, and chemotherapy, are often associated with severe side effects. In addition, tumor recurrence, metastasis, and therapy resistance are important challenges in the treatment of OSCC (56, 57). Also, the five-year survival rate of the disease has failed to improve over time (14). Therefore, targeted treatment options are being researched to reduce adverse effects and spare healthy tissue. In this study, we aimed to investigate the use of DPSC-based suicide gene therapy as a targeted therapy for OSCC.

DPSC are transduced with a polycistronic lentiviral construct, designed to express multiple genes (58). The vector contains an elongation factor-1 alpha (EF-1α) promoter, which is responsible for gene

expression of downstream genes. This promotor has a long-term stability and is one of the strongest promoters in viral vectors for human cells (59). Downstream the EF-1α promotor, the HSV1-TK gene was located. FLAG-tag, His-tag, and Fluc were linked via peptide 2A (T2A) and puromycin resistance cassette via the internal ribosome entry site (IRES). T2A and IRES allow multiple gene expression in a polycistronic vector construct (60). As mentioned earlier, the HSV1-sr39TK variant was used in this research since this variant requires a lower amount of GCV and enhances cell death and because it can be used as a reporter gene to image HSV1-TK gene expression *in vivo* (11, 39). Additionally, FLAG-tag and His-tag were used as an additional validation control for ICC. Also, ampicillin resistance (AmpR) was included in the vector for bacterial amplification of the construct.

The **first aim** of this research was to characterize HSV1-TK$^+$ DPSC and investigate interpatient variability. ICC analyses demonstrated that transduced DPSC have a significantly higher protein expression of HSV1-TK, FLAG-, and His-tag in all donors compared to non-transduced cells. Our results also indicated that the protein expression of HSV1-TK was higher than the FLAG- and His-tag genes. This observation can be explained due to the gene locations within the polycistronic vector construct. Genes located more downstream the promoter are often less expressed (61). Next, DPSC were characterized via qPCR. These results showed that HSV1-TK was expressed only in HSV1-TK$^+$ DPSC, but not in HSV1-TK$^-$ DPSC in all donors, indicating that DPSC were transduced correctly. Since the vector contained the Fluc gene, the transduction of the suicide gene was also validated via BLI. In the presence of ATP and oxygen, firefly luciferase is able to convert D-luciferin into oxyluciferin, which will result in the generation of bioluminescent signals (62). The bioluminescent signals in transduced cells were higher than in non-transduced cells (data not shown). In the future, BLI can also be used to track DPSC migration toward cancer cells in an *in vivo* study.

The difference in protein expression of transduced and non-transduced DPSC in HSV1-TK, FLAG, and His was assessed to investigate if these proteins were expressed evenly in all donors. ICC analyses indicated that there were no significant differences between patients, meaning that lentiviral transduction of the construct has no influence on the protein expression of the three genes. However, these results are contradictory to the qPCR data. HSV1-TK mRNA levels of transduced DPSC in P202 and P205 differed significantly from the mRNA levels of other patients. A possible explanation for the difference in HSV1-TK mRNA levels in P202 and P205 is that transduced DPSC may have been contaminated with non-transduced DPSC, which do not express HSV1-TK. Based on ICC and qPCR data, it can be concluded that DPSC from all donors were transduced correctly, however, it is highly recommended to treat DPSC P202 and P205 with puromycin. As described earlier, transduced DPSC contain the puromycin resistance cassette. Therefore, after treating DPSC with puromycin, non-transduced DPSC will be eliminated since it is toxic to cells (63). To investigate how many DPSC are actually transduced, a fluorescence activated cell sorting (FACS) analysis can be performed, a technique to distinguish different cell populations (64). In contrast, mRNA levels of the positive stem cell markers, CD90, CD105, and CD73 in transduced DPSC, did not show any differences compared to the non-

transduced DPSC, indicating that transduction of the vector has no influence on the stem cell characteristics. The preservation of stem cell characteristics in DPSC is crucial since they contain unique properties such as immunosuppressive properties, a great proliferation potential, and active migration toward tumor cells (52, 53). These results are in accordance with other studies that have confirmed the preservation of stem cell characteristics after lentiviral transduction in MSC (65).

To ensure the transfer of GCV from DPSC to OSCC, the presence of functional gap junctions between those two cell types is essential. Therefore, the **second aim** of this study was to investigate gap junction formation in a co-culture model of DPSC and OSCC. As described earlier, Cx43 is the most prevalent connexin in human gap junctions (31). Via ICC, the presence of membrane Cx43 between DPSC and OSCC was observed in 2D and 3D. While the expression of Cx43 indicates the potential presence of gap junctions, it does not ensure gap junction formation or functionality. In order to assemble complete functional gap junctional channels, hemi-channels, consisting of six connexin subunits, must dock to other hemi-channels of a neighboring cell (66). Therefore, additional experimental evidence is needed to confirm their functionality with for example the lucifer yellow dye assay. In this experiment, the impermeable lucifer yellow dye will be intracellularly injected via patch clamping. If gap junctions are functional, this dye will diffuse from the injected cell to neighboring cells, which can be visually seen (67).

Previous studies have shown that an increased expression of Cx43 in the primary tumor site has an inhibitory role in tumorigenesis via GJIC or C-terminal tail-mediated signaling and is therefore associated with a better prognosis. First, Cx43-GJIC facilitates the transfer of cAMP, leading to an increase in p27 levels, which is a tumor suppressor (68, 69). Second, the C-terminal tails of Cx43 can interact with β-catenin, leading to a reduced mount of free β-catenin for Wnt signaling, causing a reduced cell proliferation (70, 71). Connexins may also play a role in the efficacy of chemotherapeutics via GJIC. As described earlier, GJIC allow the transfer of ions and small molecules between cells. Therefore, chemotherapeutic compounds could also diffuse through GJIC to adjacent cells, increasing cell death via the bystander effect (72). *Shishido et al.* proved that upregulating Cx43 via PQ1 results in apoptosis in mammary carcinoma cells. This indicates that upregulation of Cx43 may potentially lead to better therapeutic outcomes (73, 74). Since Cx43 expression is reduced in OSCC, the upregulation may also be beneficial in the treatment of this disease (75).

The **third aim** was to investigate the killing efficiency of the HSV1-TK/GCV system on transduced DPSC and OSCC in a 2D and 3D co-culture model via the alamarBlue assay. After a seven day treatment of different GCV concentrations to a 2D co-culture model, it was observed that cell viability of these co-cultures decreased in a concentration-dependent manner. The killing effect of GCV was significantly observed in cells treated with a concentration above or equal to 1 µM. However, 3D co-cultures treated 14 days with GCV, revealed that only cells treated with 1000 µM differed significantly from untreated cells. A possible reason for this difference is that GCV is directly exposed to 2D cultures, whereas in 3D cultures, GCV is less easily diffused through the hydrogel. These findings

validate the killing efficiency of the HSV1-TK/GCV system. However, it is recommended to investigate cell viability of HSV1-TK$^+$/OSCC co-cultures treated with a concentration GCV ranging from 100 µM to 1000 µM in depth to specify more at which concentration the cytotoxic effect of GCV occurs. Previous research has shown that high doses of GCV are associated with cytotoxicity (76). Therefore, we also wanted to investigate the effect of different GCV concentrations on non-transduced DPSC/OSCC co-cultures. According to the alamarBlue data of 2D and 3D HSV1-TK$^-$/OSCC co-cultures which received GCV, the cell viability of the treated cells did not change significantly from the untreated cells. These results indicate that GCV concentrations below 1000 µM are not toxic for non-transduced DPSC and OSCC. However, this is in contrast with a previous study on glioma cells which has shown a cytotoxic effect of GCV from 400 µM (77). A possible explanation for this is that the sample size for this experiment was too low and has to be repeated.

CONCLUSION

In conclusion, our findings indicated that DPSC from five donors were successfully transduced with the lentiviral construct containing HSV1-TK. Furthermore, the presence of connexin 43 was observed between DPSC and OSCC, suggesting the potential formation of gap junctions between these cells. Moreover, the HSV1-TK/GCV system demonstrated the effective killing efficiency in both 2D and 3D co-culture models. These results prove that DPSC-mediated suicide gene therapy is a promising strategy for eliminating OSCC *in vitro*. Nevertheless, further research is necessary to evaluate the efficacy of this system *in vivo*.

REFERENCES

1. Cancer: World Health Organization (WHO); [cited 2023 Jun 1]. Available from: https://www.who.int/health-topics/cancer#tab=tab_1.
2. Hanahan D, Weinberg RA. The hallmarks of cancer. Cell. 2000;100(1):57-70.
3. Hanahan D, Weinberg RA. Hallmarks of cancer: the next generation. Cell. 2011;144(5):646-74.
4. Hanahan D. Hallmarks of Cancer: New Dimensions. Cancer Discov. 2022;12(1):31-46.
5. Bray F, Ferlay J, Soerjomataram I, Siegel RL, Torre LA, Jemal A. Global cancer statistics 2018: GLOBOCAN estimates of incidence and mortality worldwide for 36 cancers in 185 countries. CA Cancer J Clin. 2018;68(6):394-424.
6. Argiris A, Karamouzis MV, Raben D, Ferris RL. Head and neck cancer. Lancet. 2008;371(9625):1695-709.
7. D'Souza G, Kreimer AR, Viscidi R, Pawlita M, Fakhry C, Koch WM, et al. Case-control study of human papillomavirus and oropharyngeal cancer. N Engl J Med. 2007;356(19):1944-56.
8. Klein JD, Grandis JR. The molecular pathogenesis of head and neck cancer. Cancer Biol Ther. 2010;9(1):1-7.
9. Califano J, van der Riet P, Westra W, Nawroz H, Clayman G, Piantadosi S, et al. Genetic progression model for head and neck cancer: implications for field cancerization. Cancer Res. 1996;56(11):2488-92.
10. Tandon S, Shahab R, Benton JI, Ghosh SK, Sheard J, Jones TM. Fine-needle aspiration cytology in a regional head and neck cancer center: comparison with a systematic review and meta-analysis. Head Neck. 2008;30(9):1246-52.

11. Schwartz DL, Rajendran J, Yueh B, Coltrera M, Anzai Y, Krohn K, et al. Staging of head and neck squamous cell cancer with extended-field FDG-PET. Arch Otolaryngol Head Neck Surg. 2003;129(11):1173-8.
12. Lindel K, Beer KT, Laissue J, Greiner RH, Aebersold DM. Human papillomavirus positive squamous cell carcinoma of the oropharynx: a radiosensitive subgroup of head and neck carcinoma. Cancer. 2001;92(4):805-13.
13. Lindquist D, Romanitan M, Hammarstedt L, Nasman A, Dahlstrand H, Lindholm J, et al. Human papillomavirus is a favourable prognostic factor in tonsillar cancer and its oncogenic role is supported by the expression of E6 and E7. Mol Oncol. 2007;1(3):350-5.
14. Warnakulasuriya S. Global epidemiology of oral and oropharyngeal cancer. Oral Oncol. 2009;45(4-5):309-16.
15. Liu L, Chen J, Cai X, Yao Z, Huang J. Progress in targeted therapeutic drugs for oral squamous cell carcinoma. Surg Oncol. 2019;31:90-7.
16. Mohan SP, Bhaskaran MK, George AL, Thirutheri A, Somasundaran M, Pavithran A. Immunotherapy in Oral Cancer. J Pharm Bioallied Sci. 2019;11(Suppl 2):S107-S11.
17. Ferris RL, Blumenschein G, Jr., Fayette J, Guigay J, Colevas AD, Licitra L, et al. Nivolumab for Recurrent Squamous-Cell Carcinoma of the Head and Neck. N Engl J Med. 2016;375(19):1856-67.
18. Ho WJ, Mehra R. Pembrolizumab for the treatment of head and neck squamous cell cancer. Expert Opin Biol Ther. 2019;19(9):879-85.
19. Singh H, Patel V. Role of Molecular Targeted Therapeutic Drugs in Treatment of Oral Squamous Cell Carcinoma: Development and Current Strategies-A Review Article. Glob Med Genet. 2022;9(3):242-6.
20. Karjoo Z, Chen X, Hatefi A. Progress and problems with the use of suicide genes for targeted cancer therapy. Adv Drug Deliv Rev. 2016;99(Pt A):113-28.
21. Liu J, Zhang C, Hu W, Feng Z. Tumor suppressor p53 and its mutants in cancer metabolism. Cancer Lett. 2015;356(2 Pt A):197-203.
22. Senzer N, Nemunaitis J, Nemunaitis D, Bedell C, Edelman G, Barve M, et al. Phase I study of a systemically delivered p53 nanoparticle in advanced solid tumors. Mol Ther. 2013;21(5):1096-103.
23. Tabernero J, Shapiro GI, LoRusso PM, Cervantes A, Schwartz GK, Weiss GJ, et al. First-in-humans trial of an RNA interference therapeutic targeting VEGF and KSP in cancer patients with liver involvement. Cancer Discov. 2013;3(4):406-17.
24. Chen Y, Gao DY, Huang L. In vivo delivery of miRNAs for cancer therapy: challenges and strategies. Adv Drug Deliv Rev. 2015;81:128-41.
25. van der Meel R, Vehmeijer LJ, Kok RJ, Storm G, van Gaal EV. Ligand-targeted particulate nanomedicines undergoing clinical evaluation: current status. Adv Drug Deliv Rev. 2013;65(10):1284-98.
26. Freeman SM, Abboud CN, Whartenby KA, Packman CH, Koeplin DS, Moolten FL, et al. The "bystander effect": tumor regression when a fraction of the tumor mass is genetically modified. Cancer Res. 1993;53(21):5274-83.
27. Agard C, Ligeza C, Dupas B, Izembart A, El Kouri C, Moullier P, et al. Immune-dependent distant bystander effect after adenovirus-mediated suicide gene transfer in a rat model of liver colorectal metastasis. Cancer Gene Ther. 2001;8(2):128-36.
28. Aguilar LK, Guzik BW, Aguilar-Cordova E. Cytotoxic immunotherapy strategies for cancer: mechanisms and clinical development. J Cell Biochem. 2011;112(8):1969-77.
29. Xiao J, Zhang G, Qiu P, Liu X, Wu Y, Du B, et al. Tanshinone IIA increases the bystander effect of herpes simplex virus thymidine kinase/ganciclovir gene therapy via enhanced gap junctional intercellular communication. PLoS One. 2013;8(7):e67662.
30. Goodenough DA, Paul DL. Gap junctions. Cold Spring Harb Perspect Biol. 2009;1(1):a002576.
31. Aasen T, Mesnil M, Naus CC, Lampe PD, Laird DW. Gap junctions and cancer: communicating for 50 years. Nat Rev Cancer. 2016;16(12):775-88.
32. Portsmouth D, Hlavaty J, Renner M. Suicide genes for cancer therapy. Mol Aspects Med. 2007;28(1):4-41.

33. Kuriyama S, Masui K, Sakamoto T, Nakatani T, Kikukawa M, Tsujinoue H, et al. Bystander effect caused by cytosine deaminase gene and 5-fluorocytosine in vitro is substantially mediated by generated 5-fluorouracil. Anticancer Res. 1998;18(5A):3399-406.
34. Duarte S, Carle G, Faneca H, de Lima MC, Pierrefite-Carle V. Suicide gene therapy in cancer: where do we stand now? Cancer Lett. 2012;324(2):160-70.
35. Gallois-Montbrun S, Veron M, Deville-Bonne D. Antiviral nucleoside analogs phosphorylation by nucleoside diphosphate kinase. Mini Rev Med Chem. 2004;4(4):361-9.
36. Nevins TE, Dunn DL. Use of ganciclovir for cytomegalovirus infection. J Am Soc Nephrol. 1992;2(12 Suppl):S270-3.
37. Chen SH, Pearson A, Coen DM, Chen SH. Failure of thymidine kinase-negative herpes simplex virus to reactivate from latency following efficient establishment. J Virol. 2004;78(1):520-3.
38. Piret J, Boivin G. Resistance of herpes simplex viruses to nucleoside analogues: mechanisms, prevalence, and management. Antimicrob Agents Chemother. 2011;55(2):459-72.
39. Black ME, Kokoris MS, Sabo P. Herpes simplex virus-1 thymidine kinase mutants created by semi-random sequence mutagenesis improve prodrug-mediated tumor cell killing. Cancer Res. 2001;61(7):3022-6.
40. Yaghoubi SS, Gambhir SS. Measuring herpes simplex virus thymidine kinase reporter gene expression in vitro. Nat Protoc. 2006;1(4):2137-42.
41. Penuelas I, Mazzolini G, Boan JF, Sangro B, Marti-Climent J, Ruiz M, et al. Positron emission tomography imaging of adenoviral-mediated transgene expression in liver cancer patients. Gastroenterology. 2005;128(7):1787-95.
42. Leten C, Roobrouck VD, Struys T, Burns TC, Dresselaers T, Vande Velde G, et al. Controlling and monitoring stem cell safety in vivo in an experimental rodent model. Stem Cells. 2014;32(11):2833-44.
43. Lammers T, Kiessling F, Hennink WE, Storm G. Drug targeting to tumors: principles, pitfalls and (pre-) clinical progress. J Control Release. 2012;161(2):175-87.
44. Ginn SL, Alexander IE, Edelstein ML, Abedi MR, Wixon J. Gene therapy clinical trials worldwide to 2012 - an update. J Gene Med. 2013;15(2):65-77.
45. Thomas CE, Ehrhardt A, Kay MA. Progress and problems with the use of viral vectors for gene therapy. Nat Rev Genet. 2003;4(5):346-58.
46. Mohit E, Rafati S. Biological delivery approaches for gene therapy: strategies to potentiate efficacy and enhance specificity. Mol Immunol. 2013;56(4):599-611.
47. Dominici M. Minimal criteria for defining multipotent mesenchymal stromal cells. The International Society for Cellular Therapy position statement 2006 [cited 2023 Jun 1]. Available from: https://www.isct-cytotherapy.org/article/S1465-3249(06)70881-7/fulltext.
48. Miletic H, Fischer Y, Litwak S, Giroglou T, Waerzeggers Y, Winkeler A, et al. Bystander killing of malignant glioma by bone marrow-derived tumor-infiltrating progenitor cells expressing a suicide gene. Mol Ther. 2007;15(7):1373-81.
49. Leten C, Trekker J, Struys T, Roobrouck VD, Dresselaers T, Vande Velde G, et al. Monitoring the Bystander Killing Effect of Human Multipotent Stem Cells for Treatment of Malignant Brain Tumors. Stem Cells Int. 2016;2016:4095072.
50. Cooper K, Viswanathan C. Establishment of a mesenchymal stem cell bank. Stem Cells Int. 2011;2011:905621.
51. Staniowski T, Zawadzka-Knefel A, Skoskiewicz-Malinowska K. Therapeutic Potential of Dental Pulp Stem Cells According to Different Transplant Types. Molecules. 2021;26(24).
52. Lee S, Zhang QZ, Karabucak B, Le AD. DPSCs from Inflamed Pulp Modulate Macrophage Function via the TNF-alpha/IDO Axis. J Dent Res. 2016;95(11):1274-81.
53. Yamaza T, Kentaro A, Chen C, Liu Y, Shi Y, Gronthos S, et al. Immunomodulatory properties of stem cells from human exfoliated deciduous teeth. Stem Cell Res Ther. 2010;1(1):5.
54. Gillison ML, Chaturvedi AK, Anderson WF, Fakhry C. Epidemiology of Human Papillomavirus-Positive Head and Neck Squamous Cell Carcinoma. J Clin Oncol. 2015;33(29):3235-42.

55. Shield KD, Ferlay J, Jemal A, Sankaranarayanan R, Chaturvedi AK, Bray F, et al. The global incidence of lip, oral cavity, and pharyngeal cancers by subsite in 2012. CA Cancer J Clin. 2017;67(1):51-64.
56. Coletta RD, Yeudall WA, Salo T. Grand Challenges in Oral Cancers. Front Oral Health. 2020;1:3.
57. Shahoumi LA. Oral Cancer Stem Cells: Therapeutic Implications and Challenges. Front Oral Health. 2021;2:685236.
58. Wang X, Marchisio MA. Synthetic polycistronic sequences in eukaryotes. Synth Syst Biotechnol. 2021;6(4):254-61.
59. Wang X, Xu Z, Tian Z, Zhang X, Xu D, Li Q, et al. The EF-1alpha promoter maintains high-level transgene expression from episomal vectors in transfected CHO-K1 cells. J Cell Mol Med. 2017;21(11):3044-54.
60. de Felipe P. Polycistronic viral vectors. Curr Gene Ther. 2002;2(3):355-78.
61. Kaufman RJ, Murtha P, Davies MV. Translational efficiency of polycistronic mRNAs and their utilization to express heterologous genes in mammalian cells. EMBO J. 1987;6(1):187-93.
62. Takakura H. Molecular Design of d-Luciferin-Based Bioluminescence and 1,2-Dioxetane-Based Chemiluminescence Substrates for Altered Output Wavelength and Detecting Various Molecules. Molecules. 2021;26(6).
63. Compound Summary for CID 439530, Puromycin National Center for Biotechnology Information [cited 2023 Jun 8]. Available from: https://pubchem.ncbi.nlm.nih.gov/compound/Puromycin.
64. McKinnon KM. Flow Cytometry: An Overview. Curr Protoc Immunol. 2018;120:5 1 -5 1 11.
65. Meyerrose TE, Roberts M, Ohlemiller KK, Vogler CA, Wirthlin L, Nolta JA, et al. Lentiviral-transduced human mesenchymal stem cells persistently express therapeutic levels of enzyme in a xenotransplantation model of human disease. Stem Cells. 2008;26(7):1713-22.
66. Sohl G, Willecke K. Gap junctions and the connexin protein family. Cardiovasc Res. 2004;62(2):228-32.
67. Alberto AV, Bonavita AG, Fidalgo-Neto AA, Bercot F, Alves LA. Single-cell Microinjection for Cell Communication Analysis. J Vis Exp. 2017(120).
68. Zhang YW, Morita I, Ikeda M, Ma KW, Murota S. Connexin43 suppresses proliferation of osteosarcoma U2OS cells through post-transcriptional regulation of p27. Oncogene. 2001;20(31):4138-49.
69. Currier AW, Kolb EA, Gorlick RG, Roth ME, Gopalakrishnan V, Sampson VB. p27/Kip1 functions as a tumor suppressor and oncoprotein in osteosarcoma. Sci Rep. 2019;9(1):6161.
70. Spagnol G, Trease AJ, Zheng L, Gutierrez M, Basu I, Sarmiento C, et al. Connexin43 Carboxyl-Terminal Domain Directly Interacts with beta-Catenin. Int J Mol Sci. 2018;19(6).
71. Ai Z, Fischer A, Spray DC, Brown AM, Fishman GI. Wnt-1 regulation of connexin43 in cardiac myocytes. J Clin Invest. 2000;105(2):161-71.
72. Garcia-Rodriguez L, Perez-Torras S, Carrio M, Cascante A, Garcia-Ribas I, Mazo A, et al. Connexin-26 is a key factor mediating gemcitabine bystander effect. Mol Cancer Ther. 2011;10(3):505-17.
73. Shishido SN, Nguyen TA. Induction of Apoptosis by PQ1, a Gap Junction Enhancer that Upregulates Connexin 43 and Activates the MAPK Signaling Pathway in Mammary Carcinoma Cells. Int J Mol Sci. 2016;17(2).
74. Wu JI, Wang LH. Emerging roles of gap junction proteins connexins in cancer metastasis, chemoresistance and clinical application. J Biomed Sci. 2019;26(1):8.
75. Brockmeyer P, Hemmerlein B, Jung K, Fialka F, Brodmann T, Gruber RM, et al. Connexin subtype expression during oral carcinogenesis: A pilot study in patients with oral squamous cell carcinoma. Mol Clin Oncol. 2016;4(2):298-302.
76. He XL, Guo XJ, Qian GS, He XH, Huang GJ, Chen WZ, et al. Killing effects of ganciclovir on human pulmonary adenocarcinoma cell A549 transduced with HSV1-TK gene in vitro and in vivo. Acta Pharmacol Sin. 2001;22(10):901-6.

77. Li LQ, Shen F, Xu XY, Zhang H, Yang XF, Liu WG. Gene therapy with HSV1-sr39TK/GCV exhibits a stronger therapeutic efficacy than HSV1-TK/GCV in rat C6 glioma cells. ScientificWorldJournal. 2013;2013:951343.

Acknowledgements – I would like to thank Prof. Dr. Esther Wolfs for giving me the opportunity to perform my senior internship on this promising topic. I would especially like to thank Miss Jolien Van den Bosch for helping me to become a better scientist. I am grateful to have learned many different lab techniques and for the trust Miss Jolien Van den Bosch had in me during my internship. Miss Jolien Van den Bosch also helped a lot in improving my writing skills, for which I am very grateful. I would like to thank Jill Grondelaers, who definitely made my internship even more enjoyable. I would also like to thank all members of the FIERCE and LISSA research group for helping me during my internship and also for the nice talks. Finally, I would like to thank my family and friends for their support and motivation during my internship.

Author contributions – This project was conceived and designed by Prof. Dr. Esther Wolfs. Van den Bosch J. supervised the study. Lokmani E., Grondelaers J., and Van den Bosch J. were responsible for experiments. This paper was written by Lokmani E. and reviewed by Van den Bosch J.

SUPPLEMENTARY

Supplementary table 1: List of primary antibodies used for immunocytochemistry.

Antibody	Host species	Dilution DPSC	Dilution 2D DPSC/OSCC co-culture	Dilution 3D DPSC/OSCC co-culture	Supplier
HSV1-TK	Rabbit	1:200	N/A	N/A	Virusys Corporation
His-tag	Mouse	1:400	N/A	N/A	Invitrogen, Thermo Fisher Scientific
FLAG-tag	Mouse	1:200	N/A	N/A	Sigma-Aldrich
Cx43	Rabbit	N/A	1:1000	1:500	Abcam

HSV1-TK, Herpes Simplex Virus type 1 Thymidine Kinase; Cx43, connexin 43; DPSC, dental pulp stem cell; OSCC, oral squamous cell carcinoma.

Supplementary table 2: List of secondary antibodies used for immunocytochemistry.

Antibody	Dilution DPSC and 2D DPSC/OSCC co-culture	Dilution 3D DPSC/OSCC co-culture	Supplier
Alexa Fluor™ 555 donkey anti-rabbit	1:400	1:250	Invitrogen, Thermo Fisher Scientific
Alexa Fluor™ 555 donkey anti-mouse	1:400	N/A	

DPSC, dental pulp stem cell; OSCC, oral squamous cell carcinoma.

Supplementary table 3: List of primer sequences used for qPCR.

Gene	Forward primer (5'-3')	Reverse primer (5'-3')
CD90	AGAGACTTGGATGAGGAG	CTGAGAATGCTGGAGATG
CD105	CCACTAGCCAGGTCTCGAAG	GATGCAGGAAGACACTGCTG
CD73	CAGTACCAGGGCACTATCTGG	AGTGGCCCCTTTGCTTTAAT
CD45	ACCAGGGGTTGAAAAGTTTCAG	GGGATTCCAGGTAATTACTCC
CD34	TCTAGGCTCCAGCCAGAAAA	AAAACGTGTTGCCTTGAACC
HSV1-TK	ACGTACCCGAGCCGATGACTTAC	TACCGCACCGTATTGGCAAGTAGC
CYCA	AGACTGAGTGGTTGGATGGC	TCGAGTTGTCCACAGTCAGC
YWHZ	CTTGACATTGTGGACATCGG	TATTTGTGGGACAGCATGGA

HSV1-TK, Herpes Simplex Virus type 1 Thymidine Kinase; CYCA, cyclophilin A; YWHZ, 14-3-3 protein zeta.